Development and evaluation of a skeletal mechanism for EHN additized gasoline mixtures in Large Eddy Simulations of HCCI combustion

Journal:	*International Journal of Engine Research*
Manuscript ID	IJER-23-0088
Manuscript Type:	Standard Article
Date Submitted by the Author:	09-Mar-2023
Complete List of Authors:	Guleria, Gaurav; Stony Brook University, Mechanical Engineering Lopez-Pintor , Dario; Sandia National Laboratories California, Engine Combustion Research Dec, John; Sandia National Laboratories, Dept. 8300 Assanis, Dimitris; Stony Brook University, Mechanical Engineering; Institute for Advanced Computational Science; Advanced Energy Research and Technology Center
Keywords:	2-ethylexyl nitrate (EHN), low-temperature gasoline combustion (LTGC), gasoline skeletal mechanism, Computational Fluid Dynamics (CFD), Large Eddy Simulations (LES), EHN additized gasoline mixtures, HCCI combustion
Abstract:	Advanced Low Temperature Combustion modes, such as the Sandia proposed Additive-Mixing Fuel Injection (AMFI), can unlock significant potential to boost fuel conversion efficiency and ultimately improve the energy conversion of internal combustion engines. This is a novel improved combustion process is enabled by supplying small (less than 5%) variable amounts of autoignition improver to the fuel to enhance the engine operation and control. Common, diesel-fuel ignition-quality enhancing additive, 2-ethylexyl nitrate (EHN), is doped into gasoline to enable Sandia LTGC+AMFI combustion. This manuscript focuses on the development of a reduced sub-mechanism for EHN chemical kinetics at engine relevant conditions that is implemented into a skeletal mechanism for chemical kinetic studies of gasoline surrogate fuels. The mechanism validation utilized zero-dimensional numerical simulations and comparison to shock tube ignition-delay data of pure and EHN-doped n-heptane. Additional validation is presented with Homogeneous

	Charge Compression-Ignition (HCCI) engine data of pure and EHN-doped research-grade E10 gasoline. Then, the mechanism was deployed in a 3-D computational fluid dynamics (CFD) using Large Eddy Simulations (LES) to model the HCCI engine experiments of 0.4% vol EHN additized E10 gasoline at several equivalence ratios. Simulations showed a very good performance of the mechanism, and the model accurately reproduced a) the ignition point, b) combustion phasing, c) combustion duration and d) the peak of the heat release rates of the engine experiments. The results show that EHN promotes Low-Temperature Heat Release, ultimately driving the gasoline to autoignite at thermodynamic conditions where the fuel would not otherwise ignite. Overall, this work demonstrates a viable reduced chemical-kinetic mechanism for EHN and shows that it can be combined with a skeletal gasoline mechanism for CFD-LES analysis of well-mixed LTGC that matches well with experimental results. The CFD-LES analysis also shows the spatial distribution of EHN-fuel interactions that control the autoignition throughout the combustion chamber.
Note: The following files were submitted by the author for peer review, but cannot be converted to PDF. You must view these files (e.g. movies) online.	
Final_Manuscript.tex	

Development and evaluation of a skeletal mechanism for EHN additized gasoline mixtures in Large Eddy Simulations of HCCI combustion

Gaurav Guleria[1], Dario Lopez-Pintor[2], John E. Dec[2] and Dimitris Assanis[1,3]

Abstract

Advanced Low Temperature Combustion modes, such as the Sandia proposed Additive-Mixing Fuel Injection (AMFI), can unlock significant potential to boost fuel conversion efficiency and ultimately improve the energy conversion of internal combustion engines. This is a novel improved combustion process is enabled by supplying small (less than 5%) variable amounts of autoignition improver to the fuel to enhance the engine operation and control. Common, diesel-fuel ignition-quality enhancing additive, 2-ethylexyl nitrate (EHN), is doped into gasoline to enable Sandia LTGC+AMFI combustion. This manuscript focuses on the development of a reduced sub-mechanism for EHN chemical kinetics at engine relevant conditions that is implemented into a skeletal mechanism for chemical kinetic studies of gasoline surrogate fuels. The mechanism validation utilized zero-dimensional numerical simulations and comparison to shock tube ignition-delay data of pure and EHN-doped n-heptane. Additional validation is presented with Homogeneous Charge Compression-Ignition (HCCI) engine data of pure and EHN-doped research-grade E10 gasoline. Then, the mechanism was deployed in a 3-D computational fluid dynamics (CFD) using Large Eddy Simulations (LES) to model the HCCI engine experiments of 0.4% vol EHN additized E10 gasoline at several equivalence ratios. Simulations showed a very good performance of the mechanism, and the model accurately reproduced a) the ignition point, b) combustion phasing, c) combustion duration and d) the peak of the heat release rates of the engine experiments. The results show that EHN promotes Low-Temperature Heat Release, ultimately driving the gasoline to autoignite at thermodynamic conditions where the fuel would not otherwise ignite. Overall, this work demonstrates a viable reduced chemical-kinetic mechanism for EHN and shows that it can be combined with a skeletal gasoline mechanism for CFD-LES analysis of well-mixed LTGC that matches well with experimental results. The CFD-LES analysis also shows the spatial distribution of EHN-fuel interactions that control the autoignition throughout the combustion chamber.

Introduction

Low temperature combustion and, in particular, Homogeneous Charge Compression-Ignition (HCCI) has the potential to provide both high thermal efficiencies and also extremely low nitrogen oxides (NOx) and particulate matter (PM) emissions. However, the implementation of low temperature combustion in a production engine is limited by several challenges, including: 1) controlling the combustion timing, 2) obtaining complete combustion at low loads, 3) operating at high loads without excessive pressure rise rates, and 4) appropriate fuel specification (*1*). Substantial progress has been made in understanding the fundamentals of low temperature combustion, and various strategies have been developed and demonstrated aimed at addressing these standing challenges. However, further work is needed in this area, especially on techniques to provide fast combustion control as well as further understanding the effects of fuel properties on both combustion performance and engine-out emissions.

Gasoline is considered one of the most suitable fuels for low temperature combustion due to its high volatility that enhances mixture formation. However, the autoignition reactivity of gasoline at naturally aspirated (NA) conditions, with typical compression ratios, is too low to ignite the fuel. Traditionally, this drawback has been addressed by either air intake heating or retaining hot residual exhaust gasses, but this limits the engine load due to the lower charge density compared to that of conventional engines. Moreover, the hardware (such as intake air heaters) and controls (such as variable valve timing) required for charge

[1]Department of Mechanical Engineering, Stony Brook University, Stony Brook, NY, USA
[2]Sandia National Laboratories, Livermore, CA, USA
[3]Institute for Advanced Computational Science, Stony Brook University, Stony Brook, NY, USA

Corresponding author:
Dimitris Assanis, dimitris.assanis@stonybrook.edu

heating add complexity and cost to the engine. Although these problems can be mitigated with low-octane gasoline (*2–4*), such a gasoline will limit high-load operation where high autoignition resistance is required.

A strategy capable of providing fast combustion timing control and significantly reducing intake heating levels needed for autoignition in Low-Temperature Gasoline Combustion (LTGC) engines was lately proposed and developed by Dec and company (*5*). LTGC is a superset of HCCI that includes both well-mixed HCCI and its partially stratified variants. This technology, discussed here, previously named as Additive-Mixing Fuel Injection (AMFI), is predicated on the concept of supplying minute amounts of an ignition improver additive, which typically represents less than 1% of the fuel, into the fuel stream to adjust the autoignition reactivity of the fuel. This reduces (or removes) the amount of intake heat required for ignition, resulting in much higher charge densities, engine loads, and thermal efficiencies (due to lower heat transfer losses as well as mixture property benefits due to higher ratio of specific heats) compared to the straight fuel (*6*). Moreover, the additive amount is variable and can be rapidly changed on a cycle-by-cycle basis, and therefore providing a fast, cycle-resolved, control mechanism to alter combustion timing. The additive used in the AMFI system is 2-ethylhexyl nitrate (EHN), a well-known reactivity improver that is often used to enhance the cetane number of diesel fuel (*7–9*).

Previous studies have shown that EHN can effectively improve fuel's reactivity in HCCI-like engines. For example, Reitz and co-workers (*10–12*) demonstarted that EHN improves the autoingition reactivity of several fuels with high octane numbers, including ethanol, methanol and E10 gasoline (gasoline with $10\%_{vol}$ ethanol). Hosseini et al. (*13*) found that the Low-Temperature Heat Release (LTHR) advances when adding small amounts of EHN to a low-cetane diesel-like fuel derived from oil sands in a cooperative fuel research (CFR) engine. Ji et al. (*14, 15*) showed that EHN enhances the autoignition reactivity of regular gasoline at HCCI combustion conditions. Thus, a minute additive concentration ($\leq$ 0.4%vol) can significantly reduce the minimum intake heating and related temperature which is required to autoignite fuel, especially at NA conditions, where achieving autoignition can be additionally challenging. Ji et al. also details the presence of two-stage ignition for EHN doped gasoline at conditions under which non-additized gasoline does not show this behavior. This significanlty improved the combustion stability allows for additional retardation of the combustion timing, and therefore can contribute to substantially increasing the high load limit (30% at P_{intake} = 1.0 bar; 22% at P_{intake} = 1.3 bar). NOx emissions remained very low even though they increased in proportion to the additive concentration, with about 30% of the EHN nitrate group being converted to NOx, which falls within the literature reported values of boththe works of Ickes (*16*) and later Dempsey (*12*).

EHN decomposition has been widely studied in the past, with Pritchard (*17*) performing some of the pioneering studies. Pritchard's work identifies the cleavage of the N-O bond, which allows for the formation of the 2-ethylhexyloxy radical (EHO) and NO2, as the first step responsible for the thermal decomposition of EHN. Later, Pritchard also suggested that EHO decomposes to formaldehyde (CH2O) and 3-heptyl radical. Figure 1 shows this two-step decomposition pathway, which is widely accepted as the main EHN decomposition pathway.

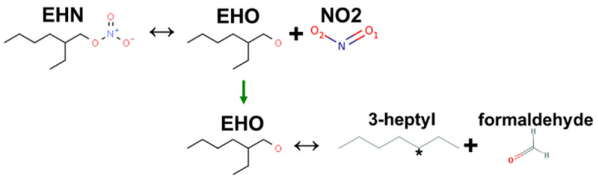

Figure 1. EHN thermal decomposition model proposed by Pritchard (*17*)

Reaction chemistry simulations of fuels additized with EHN are generally performed with the two-step chemical-kinetic mechanism shown in Figure 1 (*18–20*), and only few more comprehensive models of EHN decomposition can be found in the literature (*21*). Hartmann et al. (*18*) experimentally studied the autoignition and combustion characteristics of n-heptane doped with in both a shock tube and burner apparatus. They simulate the experiments using the two-reaction model of Figure 1 to simulate EHN unimolecular thermal decomposition, concluding that the increased reactivity of the fuel was mainly due to the 3-heptyl radical activity. Andrae (*19*) studied the impact of EHN additive on the autoignition characteristics of multiple gasoline-like surrogates by numerical simulations, in which EHN decomposition was modeled by a single reaction that forms NO2, CH2O and 3-heptyl radical. Goldsborough et al. (*20*) utilized a rapid compression machine testing facility to perform an experimental studies of two different gasoline surrogates additized with EHN. Goldsborough et al. also performed complementary modeling studies with a detailed chemical-kinetic mechanism that also featured the two-step reaction EHN model. However the EHN mechanism tended to overestimate the enhancing effect on reactivity compared to the experiments. Adhikary (*21*) developed a more sophisticated model for EHN decomposition that includes several decomposition pathways: unimolecular thermal decomposition and decomposition by radical attack. However, the model did not perform well at several conditions, especially for the negative-temperature coefficient (NTC) conditions typically reached in LTGC engines.

Lopez-Pintor and Dec (*22*) proposed a comprehensive model for EHN decomposition that accounts for three distinct EHN consumption pathways: 1) thermal decomposition, 2) radical attack and 3) ethanolysis. This three-pathway model is composed of a total of 38 species participating in 33 reactions. It was integrated into the Lawrence Livermore National Laboratory (LLNL) developed detailed chemical kinetics, hereinafter referred to as the Co-Optima 2020 mechanism (*23*), for use with gasoline surrogates. This mechanism was validated using ignition-delay data from both shock tube experiments and HCCI engine data, showing an excellent performance. This detailed EHN model can be implemented to any chemical mechanism that includes:

- Chemistry of ethanol fuel.
- Chemistry of the 3-heptyl radical (typically included in n-heptane decomposition chemistry).
- Chemistry of various short-chain hydrocarbons, such as methane, formaldehyde and propene; and active radicals such as butyl, formyl and methyl radicals.
- NOx chemistry.

However, this limits the applicability of the detailed EHN model, since many reduced mechanisms, such as those used for computational fluid dynamics (CFD), do not meet these requirements. Therefore, there is strong interest in developing a simpler but accurate chemical-kinetic model for EHN that can be implemented in reduced chemical-kinetic mechanisms for gasoline fuels to allow CFD simulations of EHN-doped fuels.

In this paper, a reduced version of the EHN mechanism developed by Lopez-Pintor and Dec (*22*) is designed and integrated in a skeletal mechanism for gasoline surrogates. After the description of the chemistry model, the reduced EHN mechanism is validated vs. additional ignition delay time data from shock tube experiments and single-cylinder HCCI engine results. Then, the mechanism is evaluated in CFD large eddy simulations (LES) of Sandia LTGC engine at HCCI-like conditions. Finally, a CFD analysis of the ignition characteristics of EHN-doped gasoline is performed.

Mechanism development

A skeletal chemical-kinetic model for the decomposition of EHN is proposed in this study. The mechanism is based on a comprehensive description of EHN chemistry developed by Lopez-Pintor and Dec (*22*), and it was designed to be implemented in a reduced chemical-kinetic mechanism already available termed SKM3.

SKM3 is a reduced mechanism for gasoline surrogates developed in a previous investigation (*24, 25*) and based on the LLNL Co-Optima detailed mechanism (*23*), one of the most sophisticated and comprehensive chemical-kinetic mechanisms for gasoline-like surrogate fuels available. Reduction of the mechanism was based on ignition-delay data obtained in a 0-D, homogeneous, closed, adiabatic and constant-volume reactor at several initial temperatures (600 – 1600 K) and pressures (1 – 50 bar) as well as equivalence ratios (0.3 – 1.5). The fuel used in this work intends to target a typical research-grade regular-octane rated E10 gasoline commonly referred to as RD5-87 (RON = 92.6, AKI = 88.5). To mimic the behavior of RD5-87, a surrogate fuel is used in this work that was previously formulated by Lopez-Pintor et al. and widely used in former investigations (*26–29*), the composition of which is shown in Table 1. Directed Relation Graph (DRG) (*30*) and DRG Aided Sensitivity Analysis (DRGASA) (*31*) methods were applied for detailed mechanism reduction, and only the chemistry of the species that compose the surrogate was included in SKM3, allowing for a more effective reduction. Chemical lumping was not considered in the reduction method. Optimization was applied to minimize the ignition-delay deviation between the detailed mechanism and SKM3. The set of ignition-delay times used for optimization was obtained at temperatures ranging from 700 K to 1100 K, with pressures ranging from 15 bar to 50 bar and with equivalence ratios ranging from 0.4 to 1.0. This range of conditions was narrower than that used for the DRG and DRGASA reduction methods due to the high computational cost of optimization. For the given components composing the surrogate fuel, only chemical reactions involving species of the same carbon number as the specific component were considered candidates for optimization. For example, for n-heptane component, that features a carbon count of 7, only reactions involving species with the same carbon of 7 were considered for optimization within the entirety of the n-heptane sub-mechanism. Reactions for optimization were identified using sensitivity analyses, with the maximum number of reactions considered for optimization equaling to exactly 30 (i.e., the 30 most sensitive reactions that affect the ignition delay period). Only the pre-exponential coefficient of the Arrhenius expression was adjusted and results were sufficiently good to not adjust the other Arrhenius coefficients. The final version of SKM3 consists of 164 species and 582 reactions.

Table 1. Composition of the gasoline surrogate for RD5-87 in mole fraction.

RD5-87 surrogate composition	
Species	Mole Fraction (%)
1-Hexene	6
Cyclo-pentane	7.0
N-heptane	9.0
N-pentane	9.0
Toluene	20.0
Ethanol	20.0
Iso-octane	29.0

Despite the fact that a complete description of the detailed EHN mechanism is given in (*22*), a brief description of the chemical pathways included in the model is given here for

the readers' convenience. Three decomposition pathways for EHN were included in the detailed EHN model:

- Unimolecular thermal decomposition (as shown in Figure 1) that includes the pressure dependency of the specific reaction rate associated with the N-O cleavage.
- Decomposition by radical attack to form alkyl oxides and nitrous species.
- Ethanolysis, which is the reaction of EHN and ethanol to form ethyl nitrate and 2-ethylexanol.

Interestingly, these pathways have EHO as the main decomposition product of EHN, so EHO chemistry has been described in detail in the mechanism. EHO decomposition was modeled by three chemical pathways:

- Oxidation by molecular oxygen, which is the initial step for the decomposition of EHO.
- Unimolecular decomposition to formaldehyde and 3-heptyl radical, which dominates at moderate-to-low temperatures (T<750 K).
- Unimolecular decomposition to butoxy dirradical and 1-butyl radical, which dominates at moderate-to-high temperatures (T>900 K).

Unfortunately, a direct implementation of this detailed EHN model in SKM3 was not possible because SKM3 does not include many of the chemical pathways required by the detailed EHN mechanism. To solve this issue, the detailed EHN model was merged with the LLNL Co-Optima 2020 gasoline surrogate mechanism (*23*) and reduced based on ignition-delay data of the surrogate fuel described in Table 1 doped with EHN additive at a rate of 1% by vol. Ignition-delay times were calculated in CHEMKIN using a 0-D, closed, adiabatic, homogeneous and constant-volume reactor at several initial temperatures (600 – 1000 K), pressures (3 – 70 bar), oxygen contents (9% - 21%) and equivalence ratios (0.2 – 1). A custom DRG-like method was used to reduce the EHN model. The starting species was selected as EHN and the worst-case ignition-delay error tolerance was set to be 15%. However, since the objective of this reduction is to obtain a skeletal model for EHN decomposition, the DRG method was allowed to reduce only the detailed EHN sub-model without modifying the LLNL Co-Optima 2020 detailed mechanism.

The resulting reduced EHN mechanism includes the pressure-dependent unimolecular decomposition of EHN via N-O bond cleavage described by the following reaction:

$$\mathrm{EHN} \longleftrightarrow \mathrm{EHO} + \mathrm{NO_2} \quad \text{(R1)}$$

However, both ethanolysis and radical attack decomposition were eliminated from the model. The reduced EHN mechanism also includes two different pathways for the decomposition of EHO, described by the following reactions:

$$\mathrm{EHO} \longleftrightarrow \mathrm{C_2H_5[CH]C_4H_9} + \mathrm{CH_2O} \quad \text{(R2)}$$

$$\mathrm{EHO} \longleftrightarrow \mathrm{C_3H_7[CH_2]} + \mathrm{C_2H_5[CH]CH_2O} \quad \text{(R3)}$$

Where R2 represents the decomposition of EHO to formaldehyde and 3-heptyl radical , whereas R3 represents the decomposition of EHO to butoxy and 1-butyl radicals. chemical-kinetic analyses showed that the butoxy diradical rapidly reacts generating propane and formaldehyde. Thus, R3 was re-written as:

$$\mathrm{EHO} \longleftrightarrow \mathrm{C_3H_7[CH_2]} + \mathrm{C_3H_6} + \mathrm{CH_2O} \quad \text{(R4)}$$

For simplicity, R4 was included in the reduced EHN mechanism instead of R3. Finally, EHO oxidation was eliminated from the model.

The chemistry of all the species that compose the reduced EHN decomposition model was already included in SKM3 with the exception of the 3-heptyl radical. Therefore, a reduced decomposition model for 3-heptyl radical, which was obtained via the reduction method explained above, was implemented in SKM3. The reduced EHN model plus the additional 3-heptyl radical chemistry were integrated in SKM3 leading to a 177 species and 595 reactions mechanism for EHN-gasoline mixtures.

Mechanism validation in 0-D simulations

Shock tube and HCCI engine data were used to validate the reduced EHN model integrated in SKM3. Simulations with the detailed EHN model implemented in the full LLNL Co-Optima 2020 mechanism were also included in this section for a better evaluation of the reduced mechanism.

Shock tube validation

Ignition-delay time shock-tube measurements, carried out by Hartmann et al. (*18*), of EHN-doped n-heptane were simulated in commercially available ANSYS CHEMKIN-PRO by using the zero-dimensional (0-D) constant volume reactor with closed, homogeneous, and, adiabatic conditions. Initial conditions for temperature and pressure for the simulations matched the experimental conditions experienced behind the reflected shock of the physical testing device. Hartmann et al. performed experiments at several initial temperatures, 40 Bar targeted compression pressure and with both pure n-heptane as well as with EHN additized n-heptane at concentrations of 1.0%w, 0.1%w and 0.01%w (where %w indicates the percentage mass of EHN that is added to the fuel). These experiments were performed at two different equivalence ratios of ϕ=1.0 and ϕ=0.5, conditions that are relevant to both LTGC as well as to stoichiometric spark-ignition combustion.

First, simulations with straight n-heptane were performed to evaluate the accuracy of the base mechanisms in which the EHN models were implemented, i.e., the full LLNL Co-Optima 2020 mechanism and the reduced SKM3 mechanism. Figure 2 shows the results for straight, unadditized, n-heptane at stoichiometric condtion of ϕ=1.0 (Figure 2(a)) and ϕ=0.5

(Figure 2(b)). Experimental data are plotted in red color, simulations with the detailed mechanism are shown in green color and simulations with the reduced mechanism are shown in blue color. The temperature range, reported by Hartmann et al. (*18*), depicted by red, dotted lines, establishes the uncertainty in the range of conditions experienced behind the reflected shock. These temperature conditions, behind the reflected shock, ultimately correspond to the initial temperature of the 0-D CHEMKIN simulations.

Simulations at ϕ=1.0 matched the experimental data for both the detailed and the reduced mechanisms. Simulations at ϕ=0.5 also showed a reasonably good agreement with shock-tube data at both, high and low temperatures. On the other hand, neither of the two mechanisms were able to accurately reproduce the Negative Temperature Coefficient (NTC) behavior of the fuel at lean, ϕ=0.5, conditions. The reasons for these observed inaccuracies fall beyond the scope of this investigation.

Then, simulations with EHN-doped n-heptane were performed to evaluate the accuracy of both the detailed and the reduced EHN models, and the results are shown in Figure 3. The results of ϕ=1.0 for 1.0%w, 0.1%w and 0.01%w EHN are shown in Figures 3(a), 3(b) and 3(c), respectively; and Figure 3(d) includes the results for ϕ=0.5 and 0.1%w EHN. Both the detailed and the reduced EHN mechanisms show a reasonably good agreement with the experimental data. Inaccuracies observed during intermediate temperatures that fall within the NTC region are consistent with values corresponding to unadditized n-heptane, which are observed in Figure 2. This strongly suggests that observed deviations are actually intrinsic to both the 2020 LLNL Co-Optima SKM3 mechanisms and thus not caused by the EHN models.

HCCI Engine Validation

Experiments carried out at the Sandia LTGC single-cylinder research engine facility were used to validate the reduced EHN mechanism at HCCI combustion engine conditions. This facility has been described in detail in numerous previous papers, such as (*6, 27, 32, 33*). Fully-premixed HCCI conditions are obtained by mixing the air and fuel in an external fuel vaporizer (electrical resistance heated) that is connected upstream of the intake plenum in the flow path. To avoid the probability of occurrence of any fuel condensation, the entire intake system (including pipes and plenum) was heated and controlled to 333 K, using an auxiliary resistive heater that was located in the intake manifold. For these experiments, a geometric compression ratio equal to 14:1 was selected. The engine was operated at 1200 rpm and NA conditions (i.e., intake pressure equal to 1.0 bar), using a research-grade, regular-octane rating E10 gasoline referred to as RD5-87-1C (RON = 90.6, AKI = 87.2). Two experimental campaigns were simulated:

- A combustion phasing sweep for pure (non-additized) RD5-87-1C at ϕ = 0.40 in which the combustion phasing was varied effectively by changing the intake temperature.
- An equivalence ratio sweep for EHN doped RD5-87-1C at a concentration of 0.4% by vol EHN. For each equivalence ratio, the intake temperature is altered until the ringing intensity (RI) is less than or equal to 3.0 MW/m^2. In this work, the RI of the experiments was calculated using the correlation developed by Eng (*34*).

Simulations of the crank-slider mechanism were conducted using the CHEMKIN to mimic the internal combustion engine cylinder compression and expansion processes of a homogeneous fuel-air mixture in a reciprocating engine. The stroke, bore and rod length of the engine and the effective compression ratio (estimated to be equal to 13.3:1 by heat release rate analysis of data under motoring conditions) were imposed to reproduce the compression-expansion process. Heat losses were included in the simulations using the Woschni correlation (*35*), of which characteristic constants were calibrated based on the heat release rate before and after the combustion. The composition of the charge mixture was obtained from the air and fuel flows, and the trapped mass of residual gases (the composition of which was estimated from exhaust emission measurements). Initial conditions for the simulations utilized the pressure, temperature and compositional conditions corresponded to the bottom dead center (BDC) piston position of the compression stroke. A complete compression-expansion process was simulated for each case. The BDC conditions have been used for the 0D simulations. However, for comparison with the CFD, the intake valve closing (IVC) conditions have been used.

It should be noted that RD5-87-1C has a lower RON than the research-grade gasoline RD5-87 used for the development of the mechanism, which has RON = 92.6 (see section $Mechanism\ development$ for details). Therefore, the surrogate fuel described in Table 1 would not be an appropriate surrogate for RD5-87-1C. To solve this issue, the composition of the surrogate was slightly adjusted to compensate for the variation in RON between RD5-87-1C and RD5-87, and the composition of the surrogate for RD5-87-1C is shown in Table 2. RON values were estimated from ignition data under RON-like conditions as described in (*36*). Thus, the temperature-pressure trajectory of the RON test which accounted for piston and flame compression on the end gas, was imposed on the 0-D closed reactor,

First, simulations with straight RD5-87-1C were carried out to evaluate the performance of the base chemical-kinetic mechanisms, i.e., the LLNL Co-Optima mechanism and the reduced SKM3 mechanism, at conditions without EHN. The results of the combustion phasing sweep with non-additized RD5-87-1C are shown in Figure 4, where experiments and corresponding uncertainty are plotted in red color, simulations with the detailed mechanism are shown in green color and simulations with the reduced mechanism are shown in blue color. In the figure, the point that 50% of the

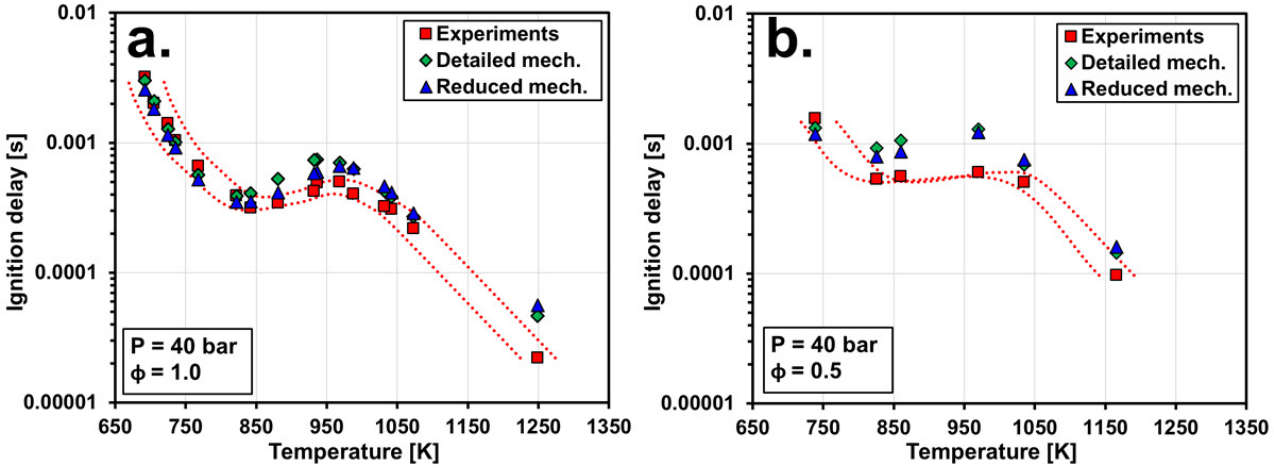

Figure 2. 0-D computed ignition-delay times of unadditized n-heptane at ϕ = 1.0 (a) and 0.5 (b), respectively, are compared against experimentally determined values. The uncertainty range in the experimentally determined temperature (uncertainty in the conditions behind the reflected shock wave) is represented by the red dotted lines.

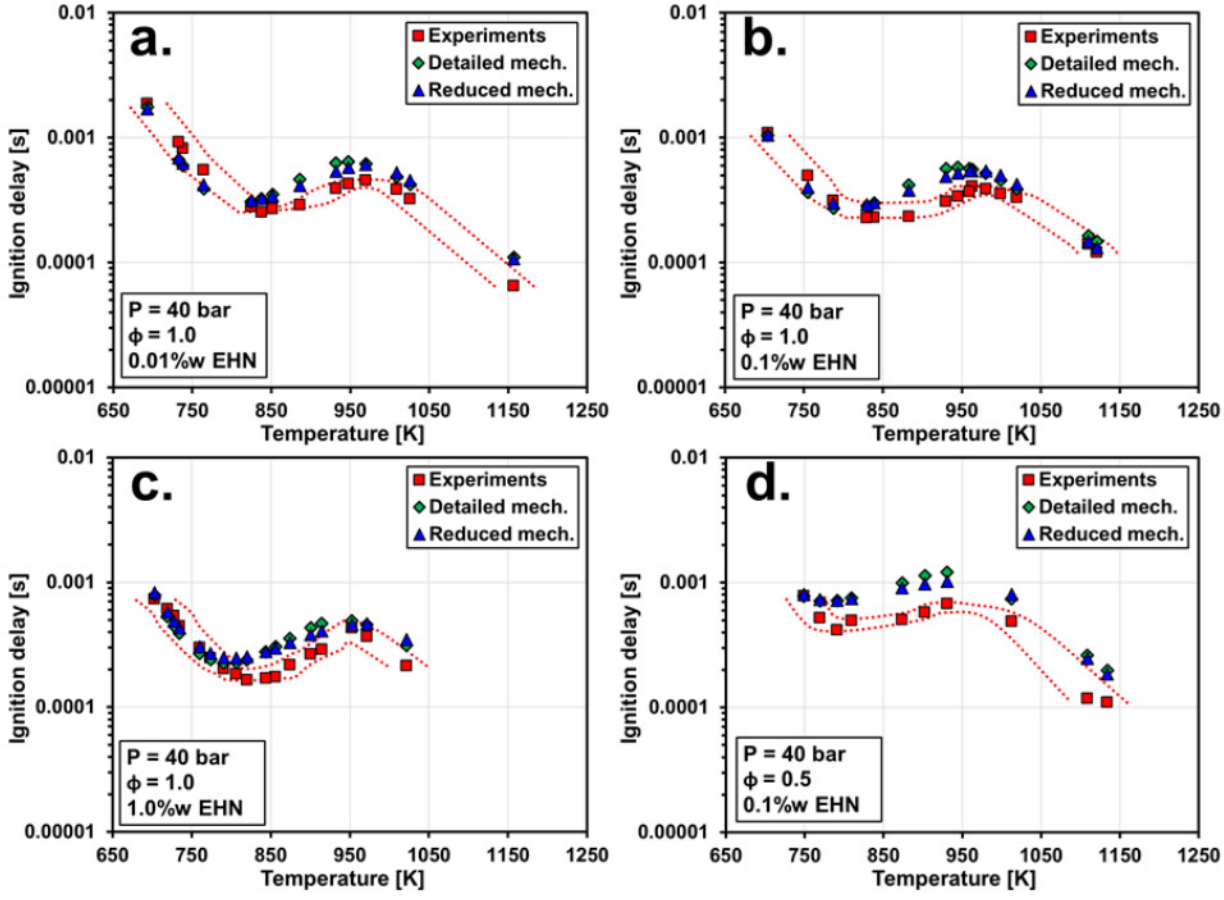

Figure 3. 0-D computed and experimental comparisons of ignition times for n-heptane additized with EHN at four conditions: P = 40 bar, ϕ = 1.0, and 0.01%w EHN (a); P = 40 bar, ϕ = 1.0, and 0.1%w EHN (b); P = 40 bar, ϕ = 1.0, and 1.0%w EHN (c), and P = 40 bar, ϕ = 0.5, and 0.1%w EHN (d).

Table 2. Composition of the gasoline surrogate for RD5-87-1C in mole fraction.

RD5-87 surrogate composition	
Species	Mole Fraction (%)
1-Hexene	6
Cyclo-pentane	7.0
N-heptane	9.0
N-pentane	11.5
Toluene	20.0
Ethanol	20.0
Iso-octane	26.5

fuel mass fraction has burned, known as CA50, is used to characterize the midpoint of the combustion phasing and the temperature at BDC-compression (T_{BDC}), is used in the x-axis. The experimental uncertainty is depicted by red, dotted lines for both the temperature at BDC-compression and the CA50. Ultimately, the numerical simulation results show a reasonably good agreement with the experimental data for these conditions.

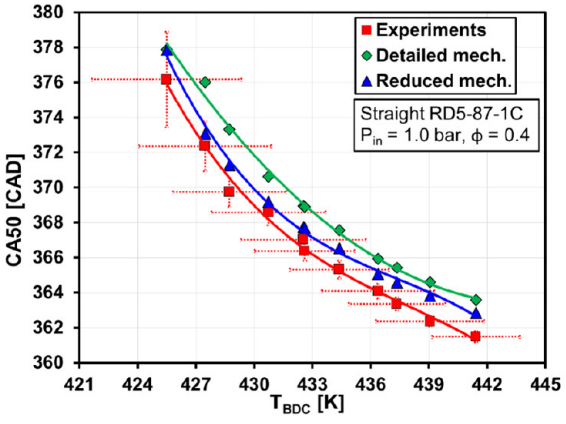

Figure 4. Experimental and simulated comparison of combustion timing sweeps versus BDC (compression stroke) temperature for non-additized RD5-87-1C at intake pressure, P_{int} = 1.0 bar and equivalence ratio, ϕ = 0.40.

Then, simulations with EHN doped RD5-87-1C, at a rate of 0.4% by vol EHN, were carried out to evaluate the performance of both the detailed and the reduced EHN models. Figure 5 shows the equivalence ratio sweep with RD5-87-1C additized with 0.4%vol EHN at 1.0 bar intake pressure and RI = 3.0 MW/m^2. In the figure, CA50 is plotted against BDC (compression stroke) temperature, which was adjusted in the experiments to obtain RI = 3.0 MW/m^2 for each equivalence ratio. The temperature at BDC-compression decreases and the CA50 retards as the equivalence ratio increases. The simulations can accurately reproduce the experiments for these conditions.

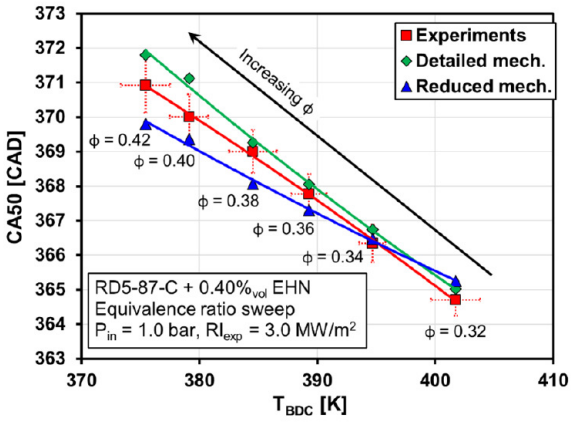

Figure 5. Experimental and simulated comparisons of combustion phasing (CA50) against BDC (compression stroke) temperatures at various equivalence ratios of RD5-87-1C additized with 0.4%vol EHN (P_{intake} = 1 bar, RI = 3.0 MW/m^2).

CFD Model development

The 3-D CFD single-cylinder engine model used in this study was set up using Converge v 2.4 (*37*) and is shown in Figure 6. The model includes three different regions, presented in order of flow direction: the intake port region (inclusive of both ports), the combustion chamber region and the exhaust port region (inclusive of both ports). The three regions of the model were each initialized using the available experimental data. The orthogonal cut cell generation method of Converge was used in combination with the fixed embedding to achieve a grid size of 0.7 mm around the valves and the combustion chamber as can be seen in Figure 7. The computational domain has approximately 3,500,000 cells at the BDC and 260,000 cells at the top dead center (TDC). The model has also been used in our previous work (*24, 28*). The combustion chamber wall temperatures were approximated by extrapolating the experimentally-measured temperatures at the fire deck (*38*). The turbulence was resolved with a Large Eddy Simulation (LES) approach that used a Dynamic Structure turbulence model with Favre filtering (*39*).

3-D CFD model utilized the SAGE detailed chemistry solver (*40*) in conjunction with the Babajimopoulos et al. (*41*) multi-zone model to accurately model combustion. The model was also setup for spray modeling in our previous work but the spray sub models were not used for the current study as the experimental data used for validation was all premixed HCCI combustion data.

The 3-D CFD model was validated using the experimental data collected at Sandia National Laboratories and presented in Figure 5, which consisted of a fully premixed set of operating conditions where the equivalence ratio (ϕ) and the intake temperature were varied together at intake pressure of 1 bar. The fuel used for these runs was RD5-87-1C which was additized with 0.4% EHN. The intake temperature

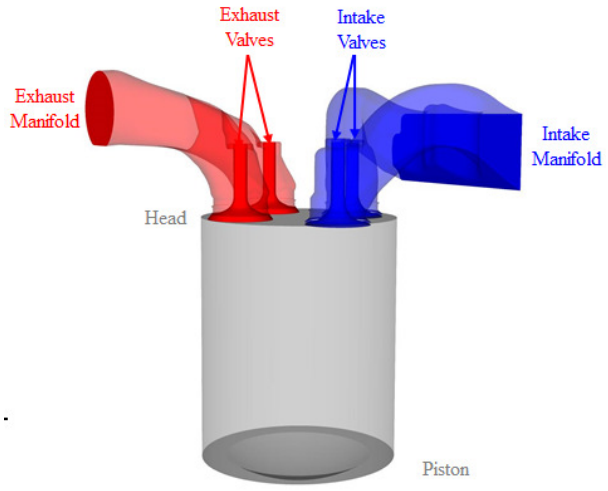

Figure 6. CFD model of the Sandia HCCI research engine showing regions; intake ports (blue), combustion chamber (gray), and exhaust ports (red).

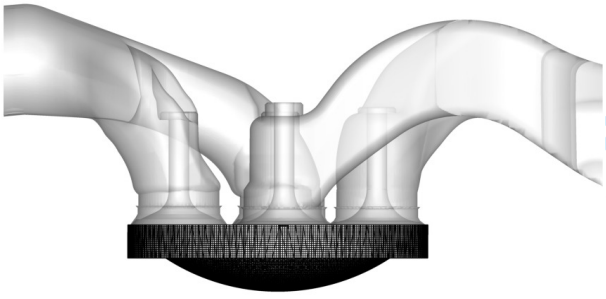

Figure 7. Isoplanar view (-20 CAD aTDC) of the Sandia HCCI research engine (MD Cummins B-Series variant) computational model.

for the simulations was adjusted to match the experimental CA50 for all the operating conditions. This approach allows to ameliorate the uncertainties in the boundary conditions and heat transfer during the intake process. The percentage temperature deviation between the experiments and model for the intake temperature and the intake valve closing (IVC) temperature is shown in Table 3. The IVC temperature comparison between the model and the experiments has been used to quantify the accuracy of the simulations. This approach has also been used in our previous work (*24*), as the IVC temperature is a much better characteristic to represent the compressed-gas temperature compared to the intake temperature due to uncertainties during the intake event. The simulations show reasonably low deviations in IVC temperature (experimental uncertainty of IVC temperature is 2%), giving confidence in the model.

In the model, seven consecutive engine cycles were run. Results of the last five cycles were compared with the experiments, whereas the first two cycles were not used in the analysis due to the impact of the initial conditions at the start of the simulation on the results. The developed 3-D CFD engine model was computed on the Stony Brook University Seawulf high performance computing (HPC) cluster (164 nodes, two CPUs per node, 14 cores per CPU). The model took approximately 14 days to run using 4 nodes (128 cores) to finish one run.

Table 3. Comparison of the percentage difference for the intake and intake valve closing temperatures between experimental engine data and model predictions.

ΔT between the experiments and CFD model				
Operating Condition (ϕ)	0.43	0.4	0.36	0.32
ΔT Intake (%)	1.6	2.3	4.7	6
ΔT IVC (%)	2.1	2.3	2.6	3.2

Results and discussion

Mechanism validation using 3-D CFD simulations

Figure 8 shows various combustion metrics obtained from experiments and compared against the model results. The results are shown for the premixed cases where the global equivalence ratio is 0.32, 0.36, 0.40 and 0.43. The experimental results used are the ensemble average of one hundred (100) consecutive cycles (blue). Error bars were obtained based on the standard deviation of the experimental data and defined as two sigma total height. The data used for the simulations is the average of five cycles (red). The combustion metrics plotted are the 10% burn point (CA10), CA50, the 90% burn point (CA90), the interval between CA10 and CA50 (CA10-50, a metric for the sequential autoingiton speed), and the interval between CA10 and CA90 (CA10-90, a metric for the total combustion duration) to determine combustion phasing as well as peak pressure, peak heat release rate and the IVC temperature to better evaluate in-cylinder thermodynamic conditions.

Figure 8 (a) shows the results for the case of ϕ = 0.32. The numerical CA10 is a little more advanced than that of the experiments. However the CA50 and CA90 values of the model and the experiments are in good agreement. The difference between the CA10-50 and CA10-90 are explained by the early CA10 of the model, which causes the observed deviation. The agreement in peak heat release rate, maximum pressure and temperature at IVC between the simulations and the experiments is also very good, and it can be said that the mechanism is able to predict the combustion for ultra lean premixed conditions accurately. Figure 8 (d) also shows a similar trend for the richest operating condition evaluated in the current study. The model predicts CA10 slightly earlier than that of the experiments. And because of that a slight deviation is observed in CA10-50 and CA10-90. However, CA50, CA90, peak heat release rate, maximum pressure and

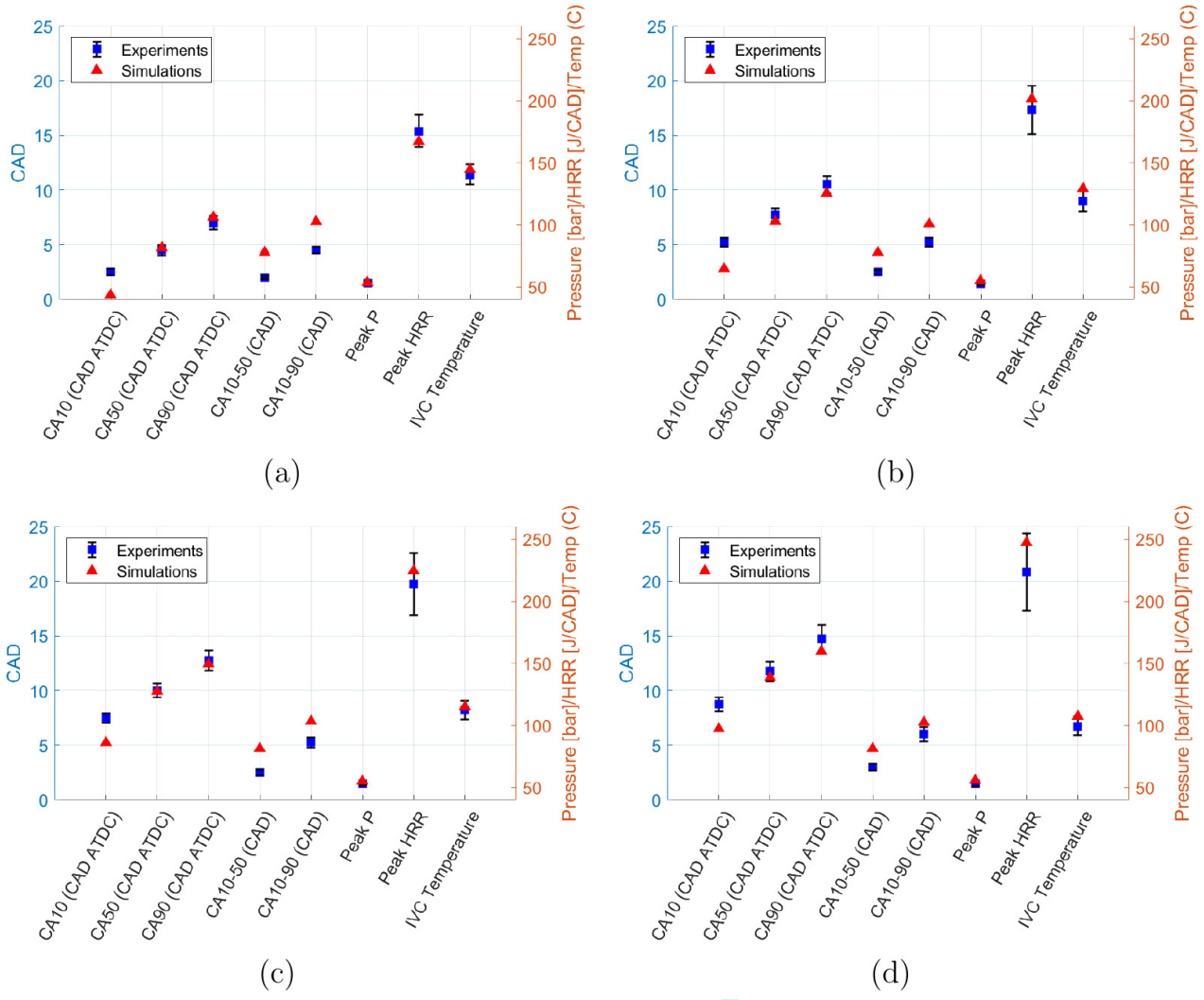

Figure 8. Experimentally determined combustion metrics (blue) are compared against corresponding simulation-derived metrics (red) for ϕ = 0.32 (a), ϕ = 0.36 (b), ϕ = 0.4 (c), and ϕ = 0.43 (d).

temperature at IVC are all predicted within the experimental uncertainty. This same behavior for CA10, CA10-50, CA10-90, CA50, and CA90 are also observed in Figures 8(b) and 8(c) for ϕ = 0.36 and 0.40, respectively.

Figure 9 shows the in cylinder pressure and heat release rates for the simulations for the premixed cases with equivalence ratio of 0.32 and 0.36 and Figure 10 shows the in cylinder pressure and heat release rates for the cases of ϕ = 0.40 and 0.43 respectively. For clarity, only twenty (20) consecutive experimental cycles are included in the figure (gray), but 100 cycles were acquired in the experiments. The last five modeled LES cycles are plotted in colored lines. It can be observed from the comparison of the experimental and modeled cycles in Figure 9 (a) that the skeletal mechanism is able to capture the pressure and heat release rates of the experiments very accurately for the operating condition of ϕ = 0.32. It can also be seen that the skeletal gasoline-EHN mechanism predicts autoignition slightly earlier compared to the experiments, in agreement with Figure 8. Figure 9(b) also shows really good agreement between the experiments and the simulations for for the operating condition of ϕ = 0.36. It can also be noted in Figure 10(a) and (b) that the gasoline-EHN skeletal mechanism is predicting the in cylinder pressure and heat release rate very accurately compared to the experiments for ϕ = 0.4 and 0.43. The LES framework of the model is suitable and tested to ensure the ability to reproduce or, at least, estimate accurately the cycle-to-cycle variability that is observed in the engine facility. The start of autoignition is predicted slightly earlier for these two operating conditions as well.

It can also be noted from Table 3 that the model is predicting the IVC temperature values within the range of 2.1% for the operating condition of ϕ=0.43 and 3.2% operating condition of ϕ=0.32. As already discussed earlier,

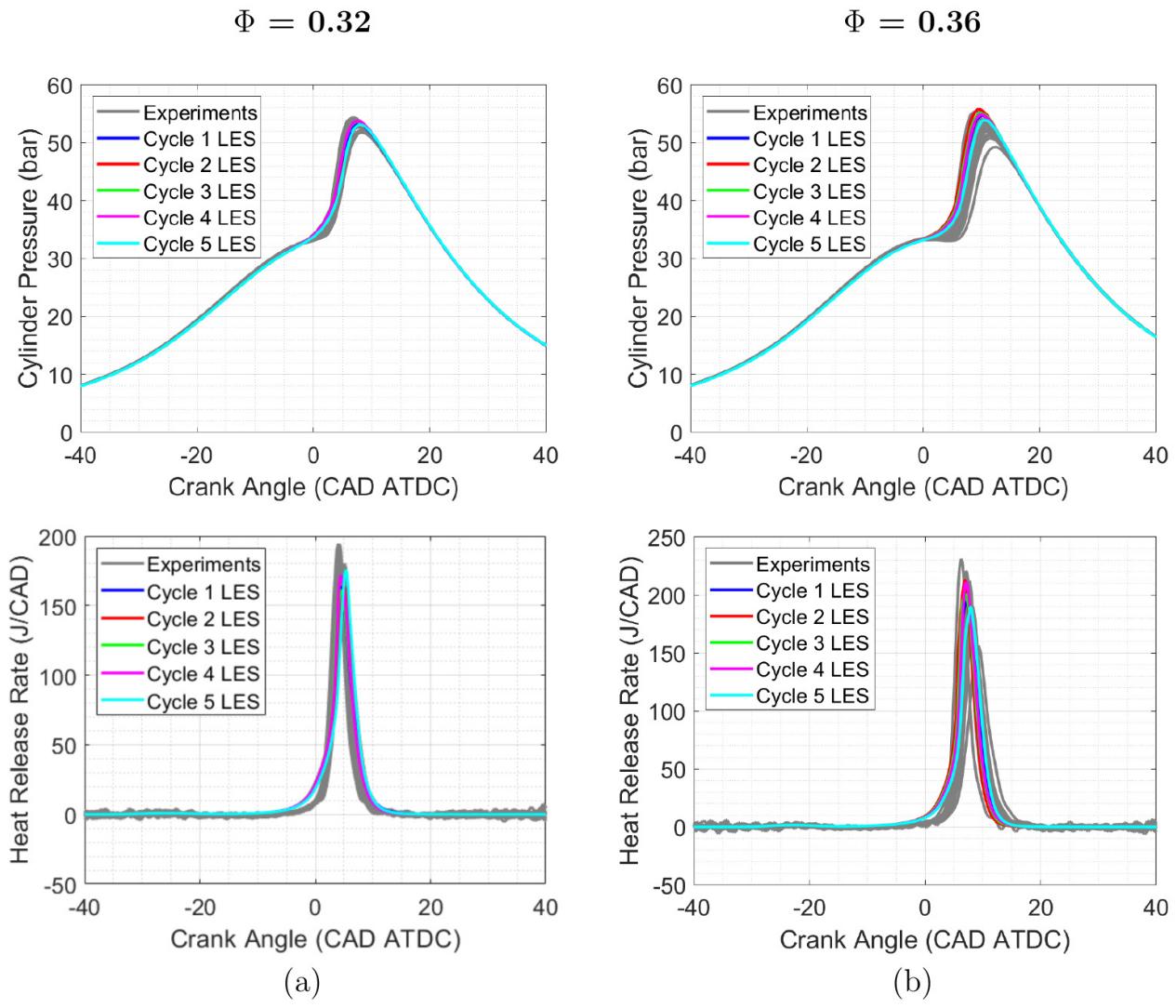

Figure 9. CFD results of the implemented SKM3-EHN mechanism at ϕ=0.32 (left) and ϕ=0.36 (right) detailed by presenting pressure (top) and heat release rates (bottom) for 5 consecutive LES cycles (colored lines) and contrasted with 20 consecutive experimental cycles (gray lines) collected at these conditions.

the IVC temperature is a much better indicator of in cylinder reactivity and the model is predicting the IVC temperature within two times the experimental uncertainty (which is 2%) as also shown in Figure 8.

Hence, the agreement of the simulations with the experiments for all the operating conditions is sufficiently good for the CFD model to be further utilized to investigate the interactions between gasoline and EHN and to analyze how these interactions can assist in controlling the ignition of additized gasoline.

Analysis of gasoline-EHN interactions

In this section the correlation between the EHN and the LTHR will be analyzed further. The modeling results from the 5^{th} cycle for the case of ϕ=0.43 will be used for the analysis. Figure11(a) shows the heat release rate for the 5^{th} modeled cycle for the case of ϕ=0.43. It is evident that a The small amount of LTHR, starting around -25 CAD aTDC, is observable. For the convenience of the reader, the zoomed in section of of the heat release plot where LTHR is starting is shown in Figure 11(b). It can be observed that the LTHR starts around -25 CAD aTDC and subsides around -10 CAD aTDC. Figure 11(c) shows the mass of EHN in the combustion chamber from -25 to -10 CAD aTDC. All the EHN in the combustion chamber is consumed during the duration of the LTHR. This co-relation between EHN and LTHR is discussed in more detail hereafter.

Figure 12 shows the visual comparison of the contours of the temperature, mass fraction of EHN and the rate of release of chemical energy for the fifth modeled cycle for

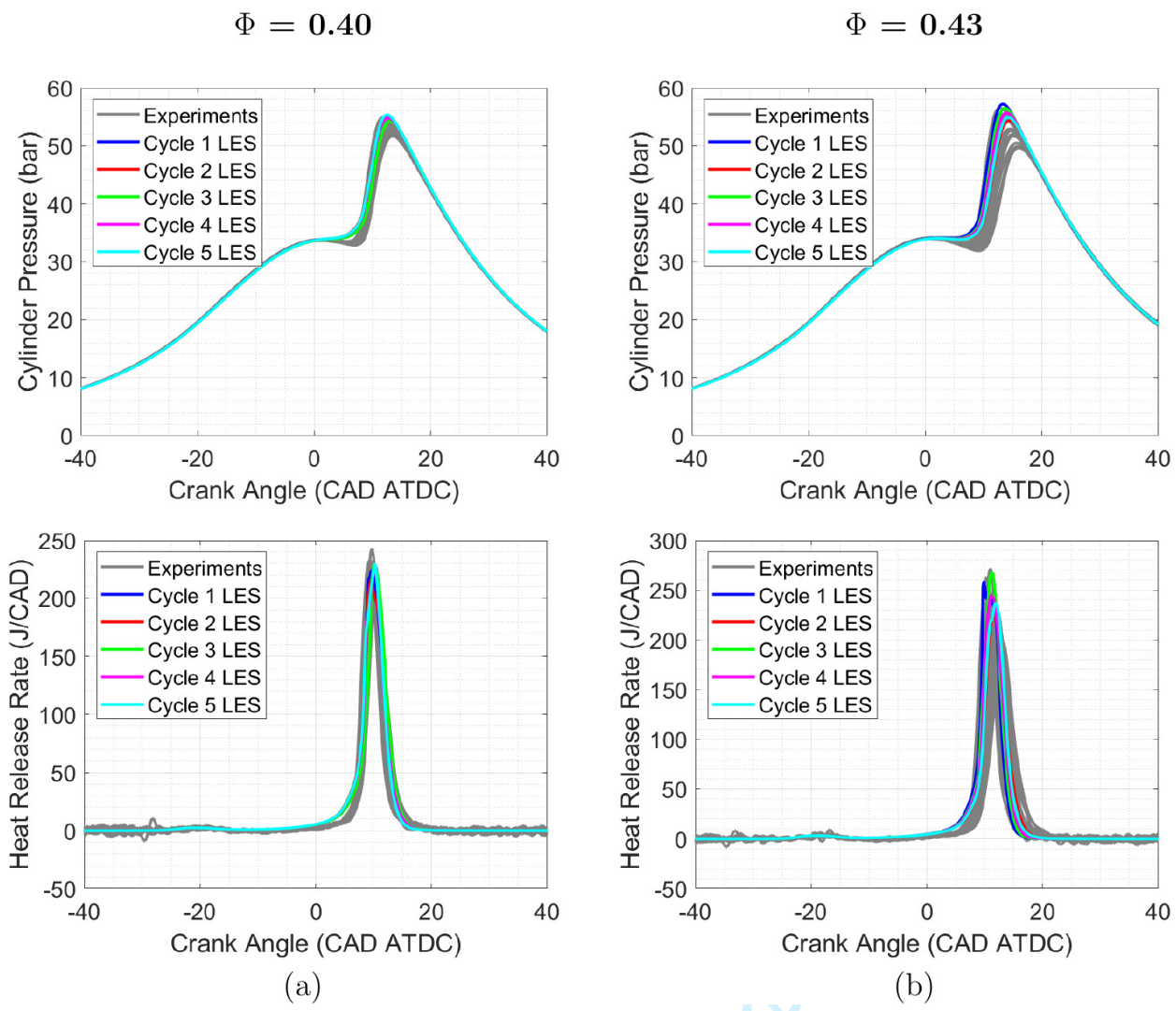

Figure 10. CFD results of the implemented SKM3-EHN mechanism at ϕ=0.40 (left) and ϕ=0.43 (right) detailed by presenting pressure (top) and heat release rates (bottom) for 5 consecutive LES cycles (colored lines) and contrasted with 20 consecutive experimental cycles (gray lines) collected at these conditions.

the operating condition of ϕ = 0.43. Converge v2.4 uses the term chemical source energy to refer to the rate of release of chemical energy which has been used in further discussion and in Figure 12. All the contours have been made using a cut plane located in the center of the combustion chamber. The left column shows the temperature contours, the middle column shows the EHN mass fraction contours and the right column shows the chemical source energy (J/s-m^3) contours at different crank angle degree values.

The CA50 is at about 6 CAD aTDC, and the images presented in the Figure are all well before TDC as the objective of the study is to find the relation between the decomposition of EHN and the LTHR, which is well before the onset of the main high-temperature heat release. The analysis is done for the crank angle values of -25 CAD aTDC, -23 CAD aTDC, -21 CAD aTDC, -19 CAD aTDC, -17 CAD aTDC and -13 CAD aTDC. The chemical source energy contours have been included in this analysis as the temperature contours alone are not a good indicator of low temperature heat release (LTHR) considering the crank angle degree duration that is being analyzed. This is due to the fact that the temperature of the combustion chamber will also be increasing due to the compression heating during the part of the cycle under consideration.

It can be observed from the first row of Figure 12 that at -25 CAD aTDC the combustion chamber temperature is around 750 K in the center of the combustion chamber and around 700 K near the walls. The middle column shows the contours for the mass fraction of EHN in the mixture and the mass fraction value is around 0.00014. It can also be observed

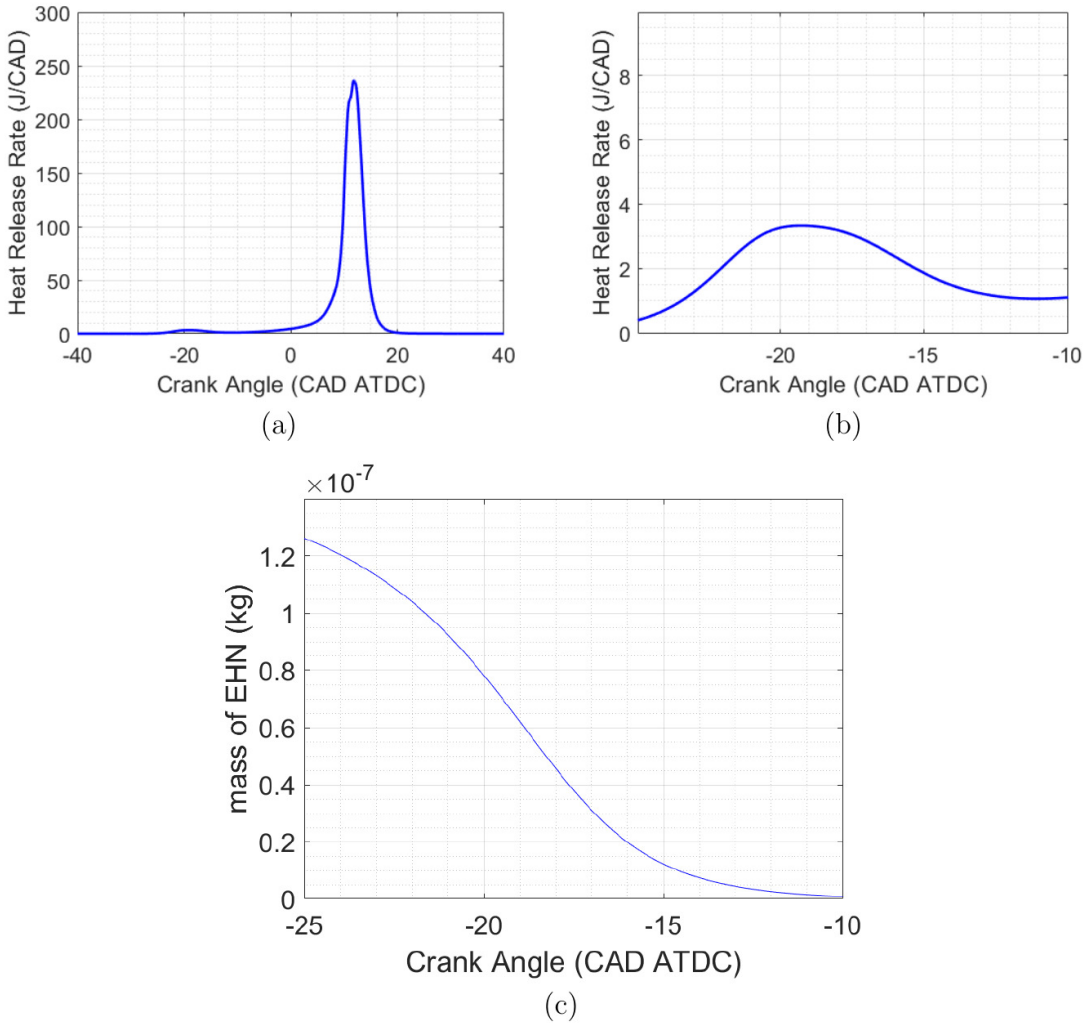

Figure 11. CFD results with SKM3-EHN mechanism (a) In-cylinder HRR (top left) (b) In-cylinder HRR zoomed in at the duration of LTHR (top right) (c) Cell averaged mass of EHN at the duration of LTHR are plotted for the 5th modeled cycle for ϕ = 0.43.

that no EHN has been consumed at -25 CAD aTDC. Finally, the plots of the right column show that there is no chemical energy released in the main chamber at -25 CAD aTDC as seen by the color of the contours of the chemical source energy.

The second row of Figure 12 similarly portrays the contours, but now at -23 CAD aTDC. The contours in the left column show that the temperature of the combustion chamber has increased to around 780 K now. It can also be observed from the middle column that the EHN present in the bulk region of the combustion chamber has started to dissociate at -23 CAD aTDC and has reduced to around around 0.00011 from around 0.00014 at -25 CAD aTDC. The right column shows that there is increase in the chemical source observed in the combustion chamber at this time step which can be seen from the color of the contour. Interestingly, the decomposition of EHN does not simultaneously occur in all parts of the combustion chamber due to the ever present effects of thermal stratification experience on the charge mixture and therefore on the decomposition of EHN. At -23 CAD aTDC, EHN from the bulk region of the chamber is already decomposing, whereas the EHN located close to the walls is not. Thus, the sequential decomposition of EHN will lead to a reactivity gradient in the chamber and, eventually, to a sequential autoingition process. This sequential EHN breakdown is in agreement with the sequential autoignition of non-additized HCCI shown in the experiments by Dec et al.(*42*)

The third row of the Figure 12 shows the contours at -21 CAD aTDC. The temperature contours here show that the combustion chamber bulk temperature increased even further to around 810 K. The middle column, representing the EHN

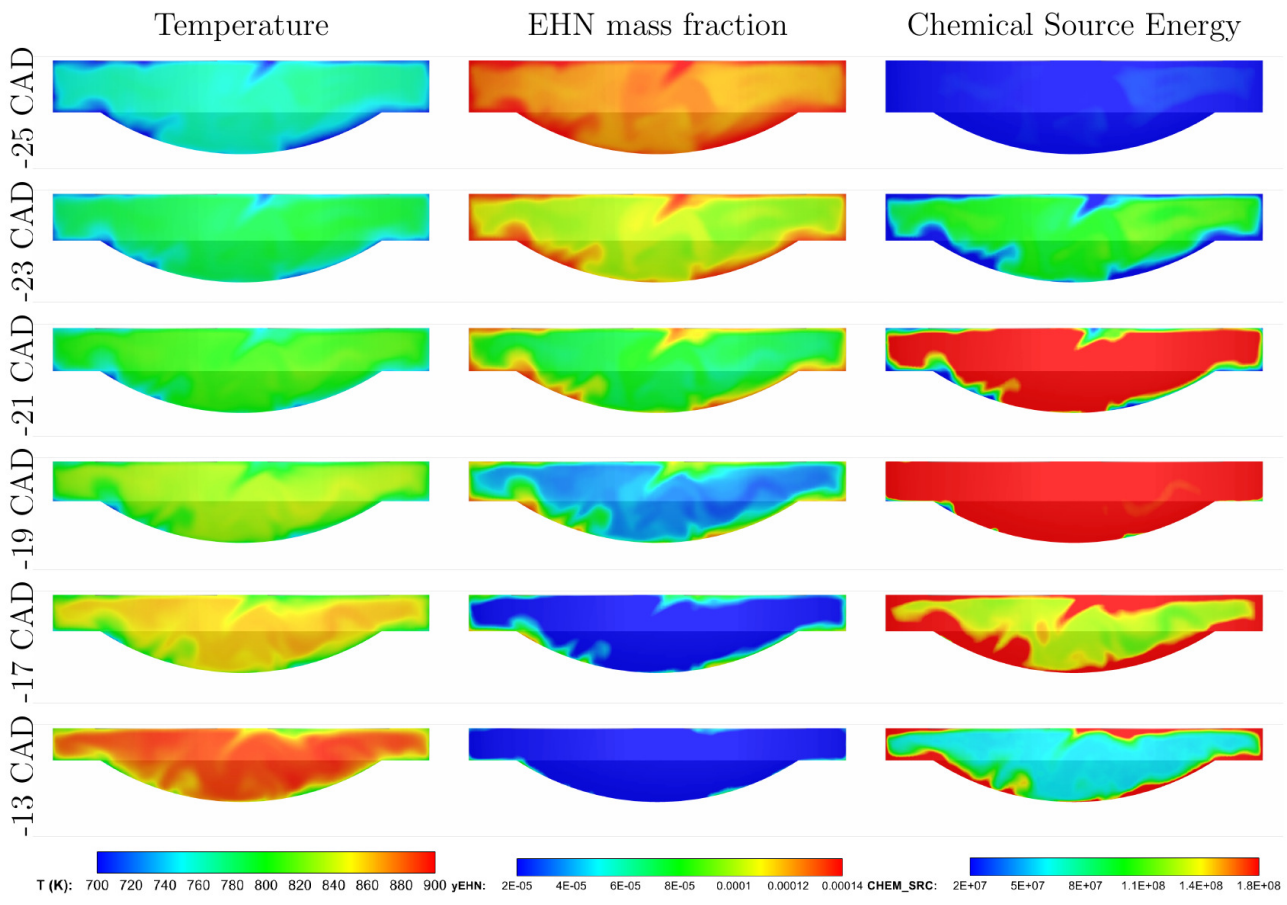

Figure 12. Contours of the temperature, EHN mass fraction and chemical source energy at –25 CAD aTDC, -23 CAD aTDC, -21 CAD aTDC, -19 CAD aTDC, -17 CAD aTDC and -13 CAD aTDC for the fifth modeled cycle for the ϕ = 0.43 operating condition

mass fraction, shows that the EHN mass fraction has further decreased as the consumption of EHN continues, promoting the start of LTHR. This effect can be observed from the chemical source energy contours as the value of the contours reach local maxima in the central core of the main chamber. The regions adjacent to the walls still have some EHN mass remaining. Another interesting observation that can be made for the EHN mass fraction and the chemical source energy contours is that the shape of both the contours is very similar for each time step analyzed, thereby indicating a correlation between the reduction in EHN mass fraction and the LTHR. This is in good agreement with the chemical-kinetic analyses presented in (*22*), which suggest that the 1-butyl and 3-heptyl radicals generated from EHN decomposition rapidly react to generate OH radicals that accelerate the chemistry associated with the low-temperature regime of the fuel and thus promotes the LTHR.

The fourth row of the Figure 12 shows the contours at -19 CAD aTDC. The temperature of the combustion chamber is still increasing rapidly at this time step. Also at -19 CAD aTDC, the EHN mass fraction has decreased considerably in the core of the combustion chamber as seen from the middle column contours. It can also be observed that the chemical source energy contours have reached local maxima in all regions of the combustion chamber. This strong correlation between events indicates that the EHN decomposition is promoting LTHR.

The fifth row of the Figure 12 shows the contours at -17 CAD aTDC. The combustion chamber temperature is still increasing has reached about 860 K. At -17 CAD aTDC most of the EHN has been consumed in the core of the chamber but some EHN remains near the wall regions as seen in the middle column. This reduction of EHN in the combustion chamber can also be seen in Figure 11(c). The chemical source energy contours show that the LTHR is subsiding in the core of the combustion chamber but it is very intense in the near-wall regions. This further suggests that the sequential decomposition of EHN caused by thermal stratification leads to a sequential autoignition process. This sequential autoignition is actually very beneficial for HCCI engine operation, since it spreads the heat release, leading

to lower peaks of pressure rise rate and allowing higher maximum engine loads.

The last row of the Figure 12 shows the contour plots at -13 CAD aTDC. The left column shows that the temperature in the combustion chamber is increasing even further due to compression heating and the remaining LTHR at this time step. The EHN in the combustion chamber has been consumed completely as seen in the middle column. And from the chemical source energy contours it can be observed that the LTHR has decreased significantly and is nearly complete. This can also be observed in Figure 11(c) where the EHN mass remaining in the cylinder at -13 CAD aTDC is around 0.005 mg. This also shows that the EHN in the cylinder was promoting exothermicity as there is still some LTHR observed at the near-wall regions in the same locations where EHN was present at -17 CAD aTDC. The results in Figure 12 demonstrate that the reduced EHN + SKM3 mechanism works well with CFD using an LES framework, providing the spatial distributions of EHN and LTHR and the important correlation between these two distributions.

Summary and Conclusions

In this investigation, a reduced EHN decomposition mechanism was developed based on a detailed model for EHN decomposition conceived by Lopez-Pintor and Dec (*22*). The mechanism was integrated in an existing reduced chemical-kinetic model for gasoline fuel termed SKM3 (*24, 25*) and validated using shock tube ignition-delay data of EHN-doped n-heptane (*18*) and HCCI engine data of EHN-doped research-grade, regular-octane rating, E10 gasoline using 0-D models. Then, the HCCI engine experiments were simulated with CFD utilizing an LES framework using SKM3 with the reduced EHN decomposition model for five sequential engine cycles. Finally, CFD analyses were performed to understand how the in-cylinder conditions affect the EHN decomposition and its effects on the fuel's autoignition reactivity.

- The combination of the reduced EHN decomposition model and the reduced SKM3 mechanism for gasoline fuel showed a very good performance, similar to that of a detailed EHN model coupled with detailed chemistry (*22*), in 0-D simulations of shock-tube and HCCI engine experiments.
- The reduced EHN-gasoline mechanism also showed very good performance when used in the 3-D CFD model with an LES framework, and the results were validated globally against the experimental data.
- The results showed that the reduced EHN-gasoline mechanism predicted the start of ignition slightly earlier than expectations based off of experimental data, but overall the combustion duration, the heat release profile, and the cycle to cycle variability as well as other combustion metrics were predicted very accurately.
- The reduced EHN-gasoline mechanism required a nominal increase in the IVC temperature to match the experimental CA50. The IVC temperatures for the simulations were in the range of 2.1% to 3.2% above the corresponding experimental IVC temperatures.
- A comparison between the temperature, EHN mass fraction and the chemical energy release rate contours show strong spatial and temporal correlations, indicating that the EHN is promoting the LTHR in the combustion chamber. This EHN effect is sensitive to the thermal stratification within the chamber, which leads to a sequential decomposition of EHN and, eventually, to a sequential autoignition process.

Acknowledgments

The authors would like to thank Tim Gilbertson, Aaron Czeszynski, Alberto Garcia and Keith Penney for their support of the Sandia HCCI Engine Laboratory. The experimental engine work was performed at the Combustion Research Facility, Sandia National Laboratories, Livermore, CA with support provided by the U.S. Department of Energy, Office of Vehicle Technologies. Sandia National Laboratories is a multi-mission laboratory managed and operated by National Technology and Engineering Solutions of Sandia, LLC., a wholly owned subsidiary of Honeywell International, Inc., for the U.S. Department of Energy's National Nuclear Security Administration under contract DE-NA0003525. The computational studies and analysis were performed at the Advanced Combustion Energy Systems Laboratory located in the Advanced Energy Research and Technology Center at Stony Brook University in Stony Brook, NY.

The authors would like to also thank Stony Brook Research Computing and Cyberinfrastructure and the Institute for Advanced Computational Science at Stony Brook University for access to the SeaWulf computing system, which was made possible by a $1.4M National Science Foundation grant (#1531492). The authors additionally thank Convergent Science for providing CONVERGE licenses and technical support for this work.

References

1. John E Dec. Advanced compression-ignition engines—understanding the in-cylinder processes. *Proceedings of the combustion institute*, 32(2):2727–2742, 2009.
2. Yi Yang, John Dec, Nicolas Dronniou, and William Cannella. Boosted HCCI combustion using low-octane gasoline with fully premixed and partially stratified charges. *SAE International Journal of Engines*, 5(3):1075–1088, 2012.
3. S Vedharaj, R Vallinayagam, Yanzhao An, M Izadi Najafabadi, Bart Somers, Junseok Chang, and Bengt Johansson. Combustion homogeneity and emission analysis during the transition

from CI to HCCI for FACE I gasoline. *SAE Technical Papers*, 2017.

4. Eshan Singh and Robert Dibble. Knock, auto-ignition and pre-ignition tendency of fuels for advanced combustion engines (FACE) with ethanol blends and similar RON. Technical Report 2020-01-0613, SAE Technical Paper, 2020.
5. John Dec and Dario Lopez Pintor. Demonstrating the potential of LTGC-AMFI to deliver the promise of low-temperature combustion. Valencia, Spain, 2020. Thermo and fluid dynamic processes in direct injection engines THIESEL.
6. Dario Lopez Pintor, Gerald Gentz, and John Dec. Mixture stratification for CA50 control of LTGC engines with reactivity-enhanced and non-additized gasoline. Technical Report 2021-01–0513, SAE Technical Paper, 2021.
7. S.N. Gadhvi. Relationship between fuel properties and cetane response of cetane improver for non-aromatic and aromatic fuels used in a single cylinder heavy duty diesel engine. *Petroleum and Chemical Industry International*, 2(1), 2019.
8. Jimmie C Oxley, James L Smith, Evan Rogers, Wen Ye, Allen A Aradi, and Timothy J Henly. Fuel combustion additives: a study of their thermal stabilities and decomposition pathways. *Energy & fuels*, 14(6):1252–1264, 2000.
9. BS Higgins, DL Siebers, and AA Aradi. Comparison of 2-ethylhexyl nitrate and fuel composition induced changes in the diesel spray ignition process. *International Journal of Engine Research*, 2(1):47–67, 2001.
10. Reed Hanson, Sage Kokjohn, Derek Splitter, and Rolf Reitz. Fuel effects on reactivity controlled compression ignition (RCCI) combustion at low load. *SAE International Journal of Engines*, 4(1):394–411, 2011.
11. John Kaddatz, Michael Andrie, Rolf D Reitz, and Sage Kokjohn. Light-duty reactivity controlled compression ignition combustion using a cetane improver. Technical Report 2012-01-1110, SAE Technical Paper, 2012.
12. Adam B Dempsey, N Ryan Walker, and Rolf Reitz. Effect of cetane improvers on gasoline, ethanol, and methanol reactivity and the implications for RCCI combustion. *SAE International Journal of Fuels and Lubricants*, 6(1):170–187, 2013.
13. V Hosseini, WS Neill, H Guo, WL Chippior, C Fairbridge, and K Mitchell. Effects of different cetane number enhancement strategies on HCCI combustion and emissions. *International Journal of Engine Research*, 12(2):89–108, 2011.
14. Chunsheng Ji, John Dec, Jeremie Dernotte, and William Cannella. Effect of ignition improvers on the combustion performance of regular-grade E10 gasoline in an HCCI engine. *SAE International Journal of Engines*, 7(2):790–806, 2014.
15. Chunsheng Ji, John Dec, Jeremie Dernotte, and William Cannella. Boosted premixed-LTGC/HCCI combustion of EHN-doped gasoline for engine speeds up to 2400 rpm. *SAE International Journal of Engines*, 9(4):2166–2184, 2016.
16. Andrew M Ickes, Stanislav V Bohac, and Dennis N Assanis. Effect of 2-ethylhexyl nitrate cetane improver on NOx emissions from premixed low-temperature diesel combustion. *Energy & Fuels*, 23(10):4943–4948, 2009.
17. HO Pritchard. Thermal decomposition of isooctyl nitrate. *Combustion and Flame*, 75(3-4):415–416, 1989.
18. M Hartmann, K Tian, C Hofrath, M Fikri, A Schubert, R Schießl, R Starke, B Atakan, C Schulz, U Maas, et al. Experiments and modeling of ignition delay times, flame structure and intermediate species of ehn-doped stoichiometric n-heptane/air combustion. *Proceedings of the Combustion Institute*, 32(1):197–204, 2009.
19. JCG Andrae. Semidetailed kinetic model for gasoline surrogate fuel interactions with the ignition enhancer 2-ethylhexyl nitrate. *Energy & Fuels*, 29(6):3944–3952, 2015.
20. SS Goldsborough, MV Johnson, C Banyon, WJ Pitz, and MJ McNenly. Experimental and modeling study of fuel interactions with an alkyl nitrate cetane enhancer, 2-ethyl-hexyl nitrate. *Proceedings of the Combustion Institute*, 35(1):571–579, 2015.
21. Bishwadipa Das Adhikary. *Low load operation in a light-duty diesel engine using high octane fuels and additives*. PhD thesis, The University of Wisconsin-Madison, 2014.
22. Dario Lopez Pintor and John Dec. Development and validation of an EHN mechanism for fundamental and applied chemistry studies. Technical Report 2022-01-0455, SAE Technical Paper, 2022.
23. Song Cheng, Chiara Saggese, Dongil Kang, S Scott Goldsborough, Scott W Wagnon, Goutham Kukkadapu, Kuiwen Zhang, Marco Mehl, and William J Pitz. Autoignition and preliminary heat release of gasoline surrogates and their blends with ethanol at engine-relevant conditions: Experiments and comprehensive kinetic modeling. *Combustion and Flame*, 228:57–77, 2021.
24. Gaurav Guleria, Dario Lopez-Pintor, John E Dec, and Dimitris Assanis. A comparative study of gasoline skeletal mechanisms under partial fuel stratification conditions using large eddy simulations. *International Journal of Engine Research*, page 14680874211031370, 2021.
25. J.M. Desantes et al. Application of a coupled eulerian spray approach and a flamelet-based combustion model to single hole primary reference fuel sprays. Zhenjiang, China, 2020. in 21st annual conference on liquid atomization and spray systems (ILASS).
26. Dario Lopez Pintor, John E Dec, and Gerald Raymond Gentz. Phi-sensitivity for LTGC engines: Understanding the fundamentals and tailoring fuel blends to maximize this property. Technical Report 2019-01-0961, SAE Technical Paper, 2019.
27. Dario Lopez-Pintor and John E Dec. Experimental evaluation of a gasoline-like fuel blend with high renewable content to simultaneously increase φ-sensitivity, ron, and octane sensitivity. *Energy & Fuels*, 35(20):16482–16493, 2021.
28. Priya Priyadarshini, Aimilios Sofianopoulos, Sotirios Mamalis, Benjamin Lawler, Dario Lopez-Pintor, and John E Dec. Understanding partial fuel stratification for low temperature gasoline combustion using large eddy simulations. *International Journal of Engine Research*, page 1468087420921042, 2020. ISSN 1468-0874.

29. Alberto Cuoci, C Thomas Avedisian, Jordan D Brunson, Songtao Guo, Alireza Dalili, Yujie Wang, Marco Mehl, Alessio Frassoldati, Kalyanasundaram Seshadri, John E Dec, et al. Simulating combustion of a seven-component surrogate for a gasoline/ethanol blend including soot formation and comparison with experiments. *Fuel*, 288:119451, 2021.
30. Tianfeng Lu and Chung K Law. A directed relation graph method for mechanism reduction. *Proceedings of the Combustion Institute*, 30(1):1333–1341, 2005.
31. Kyle E Niemeyer, Chih-Jen Sung, and Mandhapati P Raju. Skeletal mechanism generation for surrogate fuels using directed relation graph with error propagation and sensitivity analysis. *Combustion and flame*, 157(9):1760–1770, 2010.
32. Gerald Raymond Gentz, John E Dec, Dario Lopez Pintor, Jeremie Dernotte, and Chunsheng Ji. Combustion-timing control of low-temperature gasoline combustion (LTGC) engines by using double direct-injections to control kinetic rates. Technical Report 2019-01-1156, SAE Technical Paper, 2019.
33. Dario Lopez Pintor, John Dec, and Gerald Gentz. Experimental evaluation of a custom gasoline-like blend designed to simultaneously improve ϕ-sensitivity, RON and octane sensitivity. *SAE International Journal of Advances and Current Practices in Mobility*, 2(2020-01-1136):2196–2216, 2020.
34. JA Eng. Characterization of pressure waves in HCCI combustion. Technical Report 2002-01-2859, SAE Technical Paper, 2002.
35. Gerhard Woschni. A universally applicable equation for the instantaneous heat transfer coefficient in the internal combustion engine. Technical Report 670931, SAE Technical paper, 1967.
36. CK Westbrook, M Sjöberg, and NP Cernansky. A new chemical kinetic method of determining RON and MON values for single component and multicomponent mixtures of engine fuels. *Combustion and Flame*, 195:50–62, 2018.
37. KJ Richards, PK Senecal, and E Pomraning. Converge 2.4. *Convergent Science, Madison, WI (2020)*, 2020.
38. Nicolas Dronniou and John Dec. Investigating the development of thermal stratification from the near-wall regions to the bulk-gas in an HCCI engine with planar imaging thermometry. *SAE International Journal of Engines*, 5(3):1046–1074, 2012. ISSN 1946-3936.
39. Eric Pomraning. *Development of large eddy simulation turbulence models*. PhD thesis, University of Wisconsin–Madison, 2000.
40. PK Senecal, E Pomraning, KJ Richards, TE Briggs, CY Choi, RM McDavid, and MA Patterson. Multi-dimensional modeling of direct-injection diesel spray liquid length and flame lift-off length using CFD and parallel detailed chemistry. *SAE transactions*, 112(3):1331–1351, 2003. ISSN 0096-736X.
41. A Babajimopoulos, DN Assanis, DL Flowers, SM Aceves, and RP Hessel. A fully coupled computational fluid dynamics and multi-zone model with detailed chemical kinetics for the simulation of premixed charge compression ignition engines. *International journal of engine research*, 6(5):497–512, 2005. ISSN 1468-0874.
42. John E Dec, Wontae Hwang, and Magnus Sjöberg. An investigation of thermal stratification in hcci engines using chemiluminescence imaging. *SAE Transactions*, pages 759–776, 2006.